

# Serum Amyloid A3 Secreted by Preosteoclasts Inhibits Parathyroid Hormone-stimulated cAMP Signaling in Murine Osteoblasts\*

Received for publication, August 18, 2015, and in revised form, December 11, 2015. Published, JBC Papers in Press, December 23, 2015, DOI 10.1074/jbc.M115.686576

Shilpa Choudhary<sup>‡§</sup>, Alexandra Goetjen<sup>‡</sup>, Thomas Estus<sup>‡</sup>, Christian E. Jacome-Galarza<sup>¶</sup>, Hector L. Aguila<sup>¶</sup>, Joseph Lorenzo<sup>‡§</sup>, and Carol Pilbeam<sup>‡§1</sup>

From the Departments of <sup>‡</sup>Medicine and <sup>¶</sup>Immunology, <sup>‡</sup>New England Musculoskeletal Institute, University of Connecticut Health, Farmington, Connecticut 06030

**Background:** Continuous parathyroid hormone (PTH) is anabolic in cyclooxygenase-2 (Cox2) knock-out, but not WT, mice.

**Results:** Preosteoclasts secreted serum amyloid A3 (Saa3) in response to RANKL only in the presence of Cox2. Saa3 blocked PTH-stimulated cAMP production and osteoblast differentiation.

**Conclusion:** Saa3 is a novel means by which osteoclasts inhibit osteoblasts.

**Significance:** Induction of Saa3 may explain why continuous PTH causes bone loss.

Continuous parathyroid hormone (PTH) blocks its own osteogenic actions in marrow stromal cell cultures by inducing Cox2 and receptor activator of nuclear factor  $\kappa$ B ligand (RANKL) in the osteoblastic lineage cells, which then cause the hematopoietic lineage cells to secrete an inhibitor of PTH-stimulated osteoblast differentiation. To identify this inhibitor, we used bone marrow macrophages (BMMs) and primary osteoblasts (POBs) from WT and Cox2 knock-out (KO) mice. Conditioned medium (CM) from RANKL-treated WT, but not KO, BMMs blocked PTH-stimulated cAMP production in POBs. Inhibition was reversed by pertussis toxin (PTX), which blocks  $G_{\alpha_{i/o}}$  activation. Saa3 was the most highly differentially expressed gene in a microarray comparison of RANKL-treated WT versus Cox2 KO BMMs, and RANKL induced Saa3 protein secretion only from WT BMMs. CM from RANKL-stimulated BMMs with Saa3 knockdown did not inhibit PTH-stimulated responses in POBs. SAA added to POBs inhibited PTH-stimulated cAMP responses, which was reversed by PTX. Selective agonists and antagonists of formyl peptide receptor 2 (Fpr2) suggested that Fpr2 mediated the inhibitory actions of Saa3 on osteoblasts. In BMMs committed to become osteoclasts by RANKL treatment, Saa3 expression peaked prior to appearance of multinucleated cells. Flow sorting of WT marrow revealed that Saa3 was secreted only from the RANKL-stimulated B220<sup>−</sup>CD3<sup>−</sup>CD11b<sup>−/low</sup>CD115<sup>+</sup> preosteoclast population. We conclude that Saa3 secretion from preosteoclasts, induced by RANKL in a Cox2-dependent manner, inhibits PTH-stimulated cAMP signaling and osteoblast differentiation via  $G_{\alpha_{i/o}}$  signaling. The induction of Saa3 by PTH may explain the suppression of bone formation when PTH is applied continuously and may be a new therapeutic target for osteoporosis.

Parathyroid hormone (PTH)<sup>2</sup> acts on a G protein-coupled receptor (GPCR), PTH1R, to regulate calcium homeostasis and bone remodeling, stimulating both bone resorption and formation (1). PTH stimulates bone formation primarily by activating a  $G_{\alpha_s}$ -dependent cAMP/protein kinase A (PKA) signaling pathway (2). PTH stimulates bone resorption by acting on osteoblastic lineage cells to increase the expression of RANKL and decrease the expression of osteoprotegerin (OPG), a decoy receptor for RANKL (3). RANKL binds to its receptor, RANK, on monocyte-macrophage cells to promote osteoclast formation and activity. What determines the balance of PTH-stimulated resorption versus formation is still unclear. Intermittent (daily) injections of PTH are anabolic, increasing bone formation more than bone resorption, and intermittent PTH was the first anabolic therapy approved for treating osteoporosis in the United States (4, 5). Conversely, when PTH levels are continuously elevated, bone resorption is greater than bone formation and bone is lost (6–8).

PTH is a potent inducer of Cox2 in osteoblasts, and Cox2 is the major enzyme regulating the production of prostaglandins in bone (9, 10). We have previously reported that PTH infusion in mice caused persistently elevated levels of Cox2 in bone and prostaglandin E<sub>2</sub> (PGE<sub>2</sub>) (11). In Cox2 knock-out (KO) mice, PTH infusion was anabolic, increasing femoral bone mineral density, serum markers of bone formation, femoral and vertebral trabecular bone volume, cortical bone area, percent osteoblast surface, bone formation rate, and expression of genes involved in increased bone formation. In wild type (WT) mice, on the other hand, the overall effect of PTH infusion was catabolic. In contrast to the differential effects of genotype on bone

\* This work was supported, in whole or in part, by National Institutes of Health, NIAMS Grant AR060286 (to C. P.) and NIDCR Grant T90DE021 (to T. E.). The authors declare that they have no conflicts of interest with the contents of this article.

<sup>1</sup> To whom correspondence should be addressed: MC-5456, 263 Farmington Ave., CT 06030. Tel.: 860-679-3846; Fax: 860-679-1932; E-mail: pilbeam@uchc.edu.

<sup>2</sup> The abbreviations used are: PTH, parathyroid hormone; RANKL, receptor activator of nuclear factor  $\kappa$ B ligand; GPCR, G protein-coupled receptor; OPG, osteoprotegerin; PGE<sub>2</sub>, prostaglandin E<sub>2</sub>; BMSC, bone marrow stromal cell; BMM, bone marrow macrophage; CM, conditioned medium; FSK, forskolin; PTX, pertussis toxin; IBMX, isobutylmethylxanthine; POB, primary osteoblast; qPCR, quantitative PCR; TRAP, tartrate-resistant acid phosphatase; MNC, multinucleated cell; ANOVA, analysis of variance; AC, adenylyl cyclase; Fpr2, formyl peptide receptor 2; SAA, serum amyloid A; Cox, cyclooxygenase.

formation, PTH infusion increased bone resorption similarly in both WT and KO mice. These data suggest that the bone loss seen with continuously elevated PTH is largely due to suppression of bone formation and that the suppression is dependent on Cox2 expression.

We also found that in the presence of Cox2-produced PGE<sub>2</sub> *in vitro*, continuous PTH inhibits the osteoblastic differentiation of bone marrow stromal cells (BMSCs) (12). PGE<sub>2</sub> itself was not sufficient for the inhibition but required the induction or addition of RANKL. The inhibition was blocked by the addition of OPG, suggesting the involvement of bone marrow macrophages (BMMs) bearing RANK receptors that can be committed to become osteoclasts when stimulated with RANKL. Subsequently, we found that the inhibitory factor or factors were secreted from WT, but not Cox2 KO, BMMs.

The goal of the current study was to further characterize the inhibitory molecule(s) in the conditioned medium (CM). The finding that CM from RANKL-stimulated WT BMMs inhibited PTH-stimulated cAMP signaling via G $\alpha_{i/o}$  signaling, combined with a microarray analysis comparing RANKL-stimulated WT and Cox2 KO BMMs, led us to select Saa3 as a likely candidate for the inhibitory factor. Knockdown of Saa3 in BMMs and rescue with exogenous SAA confirmed this role for Saa3. In addition, dissection of bone marrow populations by fluorescence-activated cell sorting (FACS) determined that Saa3 was secreted only by the preosteoclast population. The combination of our data allows us to propose that Saa3 secreted by preosteoclasts is a novel means by which the osteoclastic lineage can inhibit PTH-stimulated osteoblastic differentiation.

## Experimental Procedures

**Materials**—Recombinant macrophage-colony stimulating factor (M-CSF), OPG/Fc-chimera, RANKL, and WRW4 (formyl peptide receptor 2, Fpr2, antagonist) were purchased from R & D Systems (Minneapolis, MN). Forskolin (FSK) and pertussis toxin (PTX) were purchased from Enzo Life Sciences (Farmingdale, NY). Human recombinant SAA (Apo-SAA), which corresponds to human Apo-SAA1 $\alpha$ , except for the presence of an N-terminal methionine and two substituted residues present in Apo-SAA2 $\beta$ , was purchased from PeproTech (Rocky Hill, NJ). PGE<sub>2</sub> and NS398, a selective inhibitor of Cox2 activity, were purchased from Cayman Chemicals (Ann Arbor, MI). Bovine PTH (bPTH 1–34), WKYMVm (a selective Fpr2 agonist), and all other chemicals were from Sigma, unless otherwise noted.

**Animals**—Mice with disruption of *Ptgs2*, which produce no functional Cox2 protein, called Cox2 KO mice, in a C57Bl/6, 129SV background were the gift of Scott Morham (13). These mice were backcrossed more than 20 generations into the outbred CD-1 background before beginning experiments. For experiments, mice were bred by crossing WT with WT and Cox2 KO with KO mice. Genotyping protocols were followed as described previously (14). To prevent genetic drift, breeding colonies were refreshed every six months by mating mice heterozygous for Cox2 with WT mice from Jackson Labs (Bar Harbor, ME). All animal studies were conducted in accordance to the approved protocols by the Animal Care and Use Committee of the University of Connecticut Health Center.

**Cell Cultures**—All cells were cultured in a humidified atmosphere of 5% CO<sub>2</sub> at 37 °C. Basic medium was  $\alpha$ -MEM (Invitrogen), 10% heat-inactivated fetal calf serum, 100 units/ml of penicillin, and 50  $\mu$ g/ml of streptomycin. The solvents used for the preparation of stock solutions of various treatments were: 0.1% bovine serum albumin (BSA) in 1 $\times$  phosphate-buffered saline (PBS) for RANKL, M-CSF, and OPG; 0.001 N hydrochloric acid in 0.1% BSA in 1 $\times$  PBS for PTH; dimethyl sulfoxide for isobutylmethylxanthine (IBMX) and FSK; water for WKYMVm and PTX; ethanol for PGE<sub>2</sub> and NS398; 25% ethanol in water for WRW4; and 5 mM Tris buffer, pH 7.6, for SAA. The concentration of all solvents in the medium was  $\leq$ 0.1%.

Primary osteoblasts (POBs) were obtained as described previously (12). For all experiments, Cox2 KO POBs were used so that there would be no contribution of PGs from osteoblasts to the cultures. Briefly, calvariae from neonatal mice were dissected, minced, washed multiple times, and digested with collagenase P and trypsin at 37 °C for 10 min to release each of fractions 1 to 4. Fraction 5 was digested for 90 min. Digest fractions 2–5 were pooled, plated at 5  $\times$  10<sup>4</sup> cells/well in 6-well dishes, and cultured in osteoblastic differentiation medium consisting of basic medium plus 50  $\mu$ g/ml of phosphoascorbate (Wako Pure Chemical Industry, Osaka, Japan). Medium was changed every 3 days. For cAMP measurement and cAMP-mediated early response gene expression studies, POBs were cultured for 5 days before treatment with antagonists and agonists. For osteoblastic differentiation studies, POBs were cultured for 14 days and all agonists and antagonists were given from the beginning of cultures and with each medium change. Five mM  $\beta$ -glycerophosphate was added on day 7 to these cultures.

BMMs were cultured as described previously (12) following the protocol of Dr. R. Faccio. Marrow was flushed from long bones, cells were counted after lysing red blood cells, and 10<sup>7</sup> nucleated cells/well were plated in 150-mm Petri dishes (Fisher Scientific, Pittsburgh, PA) in basic medium plus 100 ng/ml of M-CSF. BMMs were expanded in M-CSF two to three times, for 3 days, before being used for experiments.

**CM Experiments**—BMMs were plated at 6  $\times$  10<sup>4</sup> cells/well in 12-well dishes in basic medium plus M-CSF (30 ng/ml) with or without RANKL (30 ng/ml) for 3 days. CM was collected and centrifuged at 800 rpm for 5 min at 4 °C to remove debris and kept frozen until use. For osteoblastic differentiation studies with CM, freshly isolated Cox2 KO POBs were plated at 5  $\times$  10<sup>4</sup> cells/well in 6-well dishes and cultured for 14 days in 3 parts CM and 1 part differentiation medium plus 50 ng/ml of OPG to prevent RANKL in the CM, or induced in the POBs by PTH, from stimulating the formation of osteoclasts from any hematopoietic contaminants in these cultures. All treatments were given from the beginning of culture and with every medium change. Five mM  $\beta$ -glycerophosphate was added on day 7 to these cultures. For evaluation of cAMP-mediated early response gene expression, POBs were plated at 5  $\times$  10<sup>4</sup> cells/well in 6-well dishes and cultured for 5 days in differentiation medium. On day 5, POBs were given 50 ng/ml of OPG, 3 parts CM and 1 part differentiation medium with or without PTX (100 ng/ml) 1.5 h prior to the addition of agonists for the last 3 h. For cAMP measurement, POBs were plated similarly, cul-

## Saa3 Inhibits PTH Signaling in Osteoblasts

**TABLE 1**

Primers used to analyze gene expression by quantitative real time PCR  
Genes were analyzed by TaqMan® gene expression assay.

Gene name	TaqMan® probe number	Gene name	TaqMan® probe number
<i>Gapdh</i>	Mm99999915_g1	<i>Saa1</i>	Mm00656927_g1
<i>Ramp3</i>	Mm00840142_m1	<i>Saa2</i>	Mm04208126_mH
<i>Nurr1</i>	Mm00443060_m1	<i>Saa3</i>	Mm00441203_m1
<i>cFos</i>	Mm00487425_m1	<i>Saa4</i>	Mm04208129_m1
<i>Fpr2</i>	Mm00484464_s1	<i>Runx2</i>	Mm00501584_m1

tured for 5 days, and treated with 0.5 mM IBMX to block phosphodiesterase activity, 50 ng/ml of OPG and 3 parts CM and 1 part differentiation medium 1.5 h prior to the addition of agonists for the last 20 min.

**Intracellular cAMP Measurement**—Cells were scraped up in 400 µl/well of ice-cold ethanol. The ethanolic cell suspensions were collected and centrifuged at 1500 × g for 10 min at 4 °C. Supernatants were collected and evaporated to dryness using a lyophilizer. cAMP was measured using the enzyme immunoassay kit 581001 from Cayman Chemicals. The detection limit of this assay is 3.1 pmol/ml.

**Real-time (Quantitative) PCR Analysis**—Total RNA was extracted using TRIzol (Invitrogen) following the manufacturer's instructions. 2–5 µg of total RNA was DNase treated (Ambion, Inc., Austin, TX) and converted to cDNA by the High Capacity cDNA Archive Kit (Applied Biosystems, Foster City, CA). PCR was performed in 96-well plates. Primers for PCR were either Assays-on-Demand Gene Expression TaqMan primers (Applied Biosystems) or validated SYBR Green primers (Tables 1 and 2). *β-actin* or glyceraldehyde-3-phosphate dehydrogenase (*Gapdh*) served as the endogenous control. All primers were checked for equal efficiency over a range of target gene concentrations. Each sample was amplified in duplicate. A PCR mixture was run in an Applied Biosystems Prism 7300 Sequence Detection System instrument utilizing universal thermal cycling parameters. Data analysis was done using comparative  $C_t$  ( $\Delta\Delta C_t$ ) or the relative standard curve method. Results were reported as relative quantification values. As per the manufacturer's recommendation,  $C_t$  values above 33 were considered undetectable.

**Microarray Analysis of Gene Expression**—BMMs from WT and *Cox2* KO mice were cultured for 1 or 3 days with M-CSF (30 ng/ml) with or without RANKL (30 ng/ml). Total RNA from BMMs was column purified using the RNeasy kit (Invitrogen) and RNA quality was verified using Bioanalyzer RNA Nano Chips (Agilent Technologies, Santa Clara, CA). cRNA was prepared, labeled, and hybridized onto the Mouse-8 v2 Illumina Bead Chip (Illumina Inc. San Diego, CA) at the University of Connecticut Health Center microarray core facility. The Bead Chip was washed, stained with streptavidin-Cy3, and scanned onto the Illumina BeadArray Reader. Raw data were analyzed using the Illumina GenomeStudio software. For differential analysis, quantile normalization and Illumina custom error model were applied to compute detection  $p$  values and differential scores. Average signal intensity per treatment group for every gene in the array was obtained. Finally, the differential gene expression comparisons were reported as the ratio of average signal intensity of a gene for two comparison groups (fold-change).

**TABLE 2**

Primers used to analyze gene expression by quantitative real time PCR  
Genes were analyzed by SYBR Green validated primer sequences.

Gene Name	Primer sequence
<i>Bglap</i> (osteocalcin)	Reverse, TGG TCT GAT AGC TCG TCA CAA G Forward, CTG ACC TCA CAG ATC CCA AGC
<i>Actin</i>	Reverse, CCA GTT GGT AAC AAT GCC ATG T Forward, GGC TGT ATT CCC CTC CAT CG

**Measurement of Saa3 Protein**—For Western blot analysis, total cell lysates were obtained following the manufacturer's instructions (Cell Signaling, Danvers, MA). 20 µg of total proteins were run on 12% SDS-PAGE and transferred onto nitrocellulose membranes (Bio-Rad). Membranes were washed with 1× Tris-buffered saline (TBS), blocked in 5% (w/v) nonfat dry milk in 1× TBS containing 0.05% Tween 20 (1× TBST), and then incubated with SAA (H-84): sc-20651 rabbit polyclonal antibody (Santa Cruz Biotechnology) at 1:200 dilution in 5% (w/v) milk in 1× TBST overnight with gentle agitation at 4 °C. After washing with TBST, membranes were incubated with anti-rabbit IgG HRP-conjugated secondary antibody 7074 (Cell Signaling) at 1:1000 dilution. Signals were detected with Lumi-GLO chemiluminescent reagent 7003 (Cell Signaling). Membranes were then stripped off antibody and reprobed with *β-actin* (13E5) rabbit monoclonal antibody 4970 (Cell Signaling) at 1:1000 dilution in 5% (w/v) BSA in 1× TBST overnight at 4 °C. After washing, membranes were labeled with the same secondary antibody as above, signals were detected, and bands were scanned for images.

Saa3 in the CM of BMMs and in the serum of mice treated *in vivo* with PTH was measured by Mouse Saa3 ELISA kit (EZMSAA3–12K) (Millipore EMD, Billerica, MA). The limit of sensitivity of this assay is 0.078 µg/ml.

**Serum and Tibiae from PTH-infused Mice**—Tissues were obtained from 3-month-old male mice following 12 days of PTH infusion (40 µg/kg/day) as previously described (11). Blood was obtained by heart puncture after euthanasia with gaseous carbon dioxide and allowed to clot at room temperature. Serum was collected after centrifugation of samples at 5000 rpm for 10 min, and serum from each animal was divided into aliquots and frozen at –80 °C. In the same experiment, both tibiae were excised at the end of PTH infusion and combined for RNA. Ends of tibiae were cut off, but marrow was not flushed. Total RNA was extracted with TRIzol (Invitrogen) following the manufacturer's instructions and qPCR was performed as described above.

**Lentiviral shRNA Knockdown of Saa3 in BMMs**—Four unique 29-mer Saa3 shRNA lentiviral GFP plasmids (pGFP-C-Saa3shRNA1–4 Lenti Vectors, TL501964) and a scrambled plasmid (pGFP-C-scrambled Lenti Vector) were co-transfected with the packaging plasmids (TR30022) in HEK293T (CRL-3216, ATCC, Manassas, VA) cells following the manufacturer's instructions (Origene, Rockville, MD). Medium bearing viral particles was collected, spun down, and stored frozen until use. WT BMMs, grown for 20 h in M-CSF (30 ng/ml) or M-CSF plus RANKL (30 ng/ml), were transduced with the medium containing viral particles. After 72 h, cells were examined for GFP expression. RNA, proteins, and CM were collected from M-CSF plus RANKL-treated transduced BMMs. CM was

added to POBs to evaluate the effect on PTH-stimulated cAMP production and osteoblast differentiation.

**Co-culture Experiments**—M-CSF expanded BMMs transduced with Saa3 shRNA were co-cultured with POBs. POBs were plated at  $5 \times 10^4$  cells/well with  $5 \times 10^5$  cells/well of BMMs (1:10) in 6-well dishes and cultured in osteoblastic differentiation medium. All treatments were given from the beginning of culture and with every medium change. Five mM  $\beta$ -glycerophosphate was added on day 7 to these cultures.

**Flow Sorting of Whole Marrow**—All antibodies used for sorting of mouse bone marrow into different hematopoietic populations were purchased from e-Biosciences (San Diego, CA). These included anti-B cell lineage mAb (antiCD45R/B220; 47-0452), anti-T-cell lineage mAb (anti-CD3; 47-0032), anti-monocyte/macrophage antibody (anti-CD11b/Mac-1; 48-0112), and anti-cfms/CD115 antibody (13-1152). Whole bone marrow was flushed from both tibiae and femurs of mice with 10 ml of staining medium containing  $1 \times$  Hank's balanced salt solution, 10 mM HEPES, and 2% newborn calf serum. Cells were spun down at 1500 rpm for 5 min at 4 °C, supernatant was removed, and the pellet containing leukocytes and red blood cells was incubated in 1 ml of red blood lysing buffer for 5 min. The pellet was then washed in staining medium. The final pellet was suspended in 10 ml of staining medium, filtered through a 100- $\mu$ m membrane to get a single cell suspension, and cells were counted. All antibodies were titrated for optimal dilutions. Staining of cells for cell sorting was performed by standard staining procedures (15). All staining was done on ice, and dead cells were excluded by their ability to incorporate propidium iodide. Flow sorting was performed in a BD-FACS Aria (BD Biosciences, San Jose, CA) equipped with 5 lasers and 18 detectors at the University of Connecticut Health Center flow cytometry facility. Marrow was first sorted for B220<sup>+</sup> CD3<sup>+</sup> or lymphoid population (population 1) and B220<sup>−</sup> CD3<sup>−</sup> CD11b<sup>−/low</sup> or triple negative monocyte-macrophage population (population 2). Population 2 was further sorted for the absence or presence of CD115 (the receptor for M-CSF, cfms) into populations 3 (triple negative CD115<sup>−</sup>, non-M-CSF responding) and 4 (triple negative CD115<sup>+</sup>, M-CSF responding macrophage-dendritic-osteoclast progenitor population). All data were analyzed using FlowJo software from Tree Star Inc. (Ashland, OR). After sorting, populations 1 (B220<sup>+</sup> CD3<sup>+</sup>), 3 (triple negative CD115<sup>−</sup>), and 4 (triple negative CD115<sup>+</sup>) were collected and used for further study. These populations were plated at  $0.5 \times 10^5$  cells/well in 12-well dishes with M-CSF (30 ng/ml) and with or without RANKL (30 ng/ml) and grown for 3–4 days. Both RNA and CM were collected on day 3. CM was spun down and kept frozen until use.

**Tartrate-resistant Acid Phosphatase (TRAP) Staining**—Cells were fixed with 2.5% glutaraldehyde in PBS for 30 min at room temperature and stained with the Leukocyte Acid Phosphatase Kit (Sigma) following the manufacturer's instructions. Osteoclast-like cells, identified as TRAP<sup>+</sup> multinucleated cells (MNCs) with more than 3 nuclei, were counted.

**Statistics**—All data are presented as mean  $\pm$  S.E. Analysis was performed using SigmaPlot 11.0 (Systat Software, Inc.). Normally distributed data with a single independent variable were examined by one-way ANOVA and those with multiple

independent variables were examined by two-way ANOVA. Post hoc analysis was done by Bonferroni pairwise multiple comparisons. If the data for one-way ANOVA were not normally distributed, they were examined by one-way ANOVA on Ranks, followed by Dunn's test for all pairwise multiple comparisons. If the data for two-way analysis were not normally distributed, they were transformed (log 10) before analysis.

## Results

**CM from RANKL-stimulated WT, but Not Cox2 KO, BMMs Inhibited PTH-stimulated cAMP Responses in POBs in a PTX-reversible Manner**—We previously reported that CM from RANKL-stimulated WT BMMs, expressing *Cox2*, could inhibit PTH-stimulated POB differentiation (12). There was no inhibitory effect on PTH-stimulated osteoblastic differentiation if the CM came from *Cox2* KO BMMs. Many studies suggest that PTH mediates its osteogenic effects *in vitro* or its anabolic effects *in vivo* largely via  $G\alpha_s$ -cAMP-dependent protein kinase A (PKA) signaling (2, 16, 17). Therefore, we examined the effect of inhibitory CM on PTH-stimulated cAMP signaling in POBs. Because we previously found that extensive washing in the preparation of POBs did not remove all hematopoietic contaminants, which could develop into osteoclast-like cells in response to RANKL (12), we added OPG to all POB cultures to prevent osteoclastogenesis secondary to the RANKL in the CM or PTH-stimulated RANKL expression in POBs.

In the presence of CM from RANKL-treated *Cox2* KO BMMs, PTH markedly stimulated cAMP production in POBs, but CM from RANKL-treated WT BMMs blocked the PTH stimulation of cAMP production (Fig. 1A). We examined effects of PTH on the expression of several early response genes that are induced via the cAMP pathway-receptor activity modifying protein-3 (*Ramp3*) (18), *cFos* (19), and *Nurr1* (20). CM from RANKL-treated WT, but not KO, BMMs blocked the PTH induction of all these genes (Fig. 1, B–D). Consistent with our previous findings (12), CM from WT BMMs treated with M-CSF alone did not inhibit PTH-stimulated cAMP responses, and addition of RANKL was necessary for production of the inhibitory CM (Fig. 1B).

To determine whether WT CM inhibited PTH-stimulated cAMP responses at the level of the receptor for PTH (PTH1R), we treated POBs with FSK. FSK acts independently of receptors to directly activate all adenylyl cyclases (ACs) except AC 9 (21, 22). We found that FSK-stimulated *Ramp3* expression was inhibited by WT, but not *Cox2* KO, CM (Fig. 1E). Hence, the inhibitory effect was not specific for the PTH1R.

To explore a role for  $G\alpha_{i/o}$  subunits, which can inhibit AC activity and thus cAMP signaling, we treated cultures with PTX. PTX catalyzes the ADP-ribosylation of the  $G\alpha_{i/o}$  subunits, leaving them in the GDP-bound inactive state (23). ACs 1, 5, and 6 are known to be inhibited by  $G\alpha_{i/o}$  and sensitive to PTX (24). PTX alone had no significant effect on basal *Ramp3* expression or on the stimulation of *Ramp3* in response to FSK or PTH in the presence of *Cox2* KO CM. However, PTX abrogated the inhibitory effect of WT CM on both FSK- and PTH-stimulated *Ramp3* expression as shown in Fig. 1, E and F, respectively.

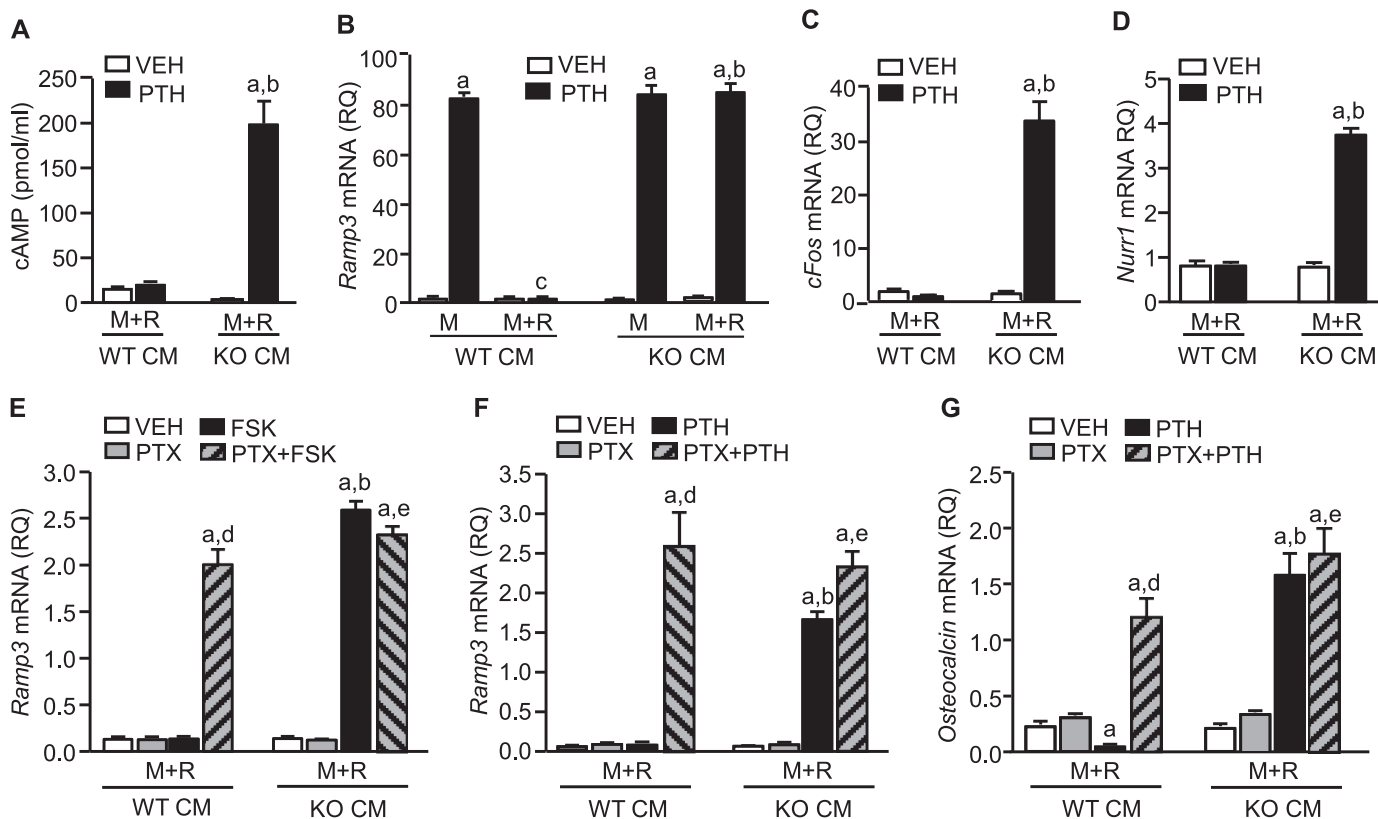


**FIGURE 1. WT CM inhibited PTH-stimulated cAMP responses and osteoblast differentiation in POBs and the inhibition was blocked by PTX.** All experiments used *Cox2* KO POBs. CM collected from M-CSF (M, 30 ng/ml) or M-CSF and RANKL (M+R, each 30 ng/ml) treated WT or *Cox2* KO BMMs was added to POBs in the ratio of 3 parts CM to 1 part differentiation media. All cultures were given OPG (50 ng/ml) at the time CM was added to prevent formation of osteoclast-like cells during treatment. For measurement of cAMP and cAMP-mediated gene expression, POBs were cultured for 5 days and then given CM 1.5 h prior to addition of agonists. **A**, cAMP production in POBs treated with 0.5 mM IBMX 1.5 h prior to addition of vehicle (VEH) or PTH (10 nM) for 20 min. **B**, *Ramp3* mRNA expression in POBs treated with VEH or PTH for 3 h. mRNA expression was measured by qPCR. **C**, *cFos* and **D**, *Nurr1* mRNA in POBs treated with VEH or PTH for 3 h. **E**, *Ramp3* mRNA in POBs treated with forskolin (FSK, 1  $\mu$ M), or F, PTH for 3 h. PTX (100 ng/ml) was added 1.5 h prior to addition of VEH or agonists. **G**, *Osteocalcin* mRNA expression in POBs treated with VEH or PTH  $\pm$  PTX (50 ng/ml) for 14 days. Bars are mean  $\pm$  S.E. for  $n = 3$  independent samples, each with 2 technical replicates. Each experiment was performed twice, except the experiment in **E**. **a**, significant effect of treatment compared with VEH control,  $p < 0.01$ . **b**, significant effect of KO CM,  $p < 0.01$ . **c**, significant effect of RANKL,  $p < 0.01$ . **d**, significantly different from PTX or PTH alone,  $p < 0.01$ . **e**, significantly different from PTX alone,  $p < 0.01$ . RQ, relative quantification values.

We previously showed that CM from RANKL-stimulated WT BMMs inhibited PTH-stimulated osteoblast differentiation as measured by *Osteocalcin* expression (12). To assess the effects of PTX on PTH-stimulated differentiation, we treated POBs with PTH plus/minus PTX for 14 days (Fig. 1G). As expected, PTH stimulated *Osteocalcin* expression in POBs cultured with KO, but not WT, CM. PTX alone had no effect on differentiation. However, the inhibitory effect of WT CM on PTH-stimulated *Osteocalcin* was abrogated by PTX. These data suggest that *Cox2*-expressing BMMs stimulated with RANKL secrete a factor that acts on osteoblasts via GPCR- $G\alpha_{i/o}$  signaling to inhibit PTH-stimulated AC/cAMP signaling and osteoblast differentiation.

**RANKL-stimulated WT, but Not *Cox2* KO BMMs, Express and Secrete *Saa3***—To compare RANKL-stimulated gene expression in WT and *Cox2* KO BMMs, we performed two independent gene expression microarrays. Each treatment group had 3–4 replicates. Data were analyzed as the ratio of average signal intensity of a gene in one group compared with the average signal intensity of the gene in the other group (fold-increase). In the first experiment, we treated for 1 day and compared differential expression in: (a) WT BMMs versus *Cox2* KO

BMMs, both treated with M-CSF and RANKL, and (b) WT BMMs treated with M-CSF and RANKL versus WT BMMs treated with M-CSF alone. In (a), *Saa3* was the most highly differentially increased gene at 207-fold. In (b), *Saa3* was the second most highly differentially increased gene at 163-fold. In the second experiment, all groups were treated with M-CSF and RANKL for 3 days. We compared (a) WT BMMs to *Cox2* KO BMMs; (b) WT BMMs treated with vehicle to WT BMMs treated with an inhibitor of *Cox2* activity (NS398, 0.1  $\mu$ M); and (c) KO BMMs treated with PGE<sub>2</sub> (1  $\mu$ M) to KO BMMs treated with vehicle. *Saa3* was the most highly differentially expressed gene in (a) 30-fold, and (c) 62-fold, and the second most highly differentially expressed gene in (b) 27-fold. Thus, the data suggested that *Saa3* expression was induced by RANKL in a *Cox2*/PGE<sub>2</sub>-dependent manner.

We validated *Saa3* gene and protein expression in WT and *Cox2* KO BMMs cultured with M-CSF alone or with M-CSF and RANKL (Fig. 2, A–C). *Saa3* gene expression on day 1 of culture measured by qPCR was undetectable ( $C_t$  values  $>33$ ) or barely detectable ( $C_t$  values of 32) in all groups except for WT BMMs treated with M-CSF and RANKL (Fig. 2A). Consistent with the mRNA expression of *Saa3*, *Saa3* protein expression on

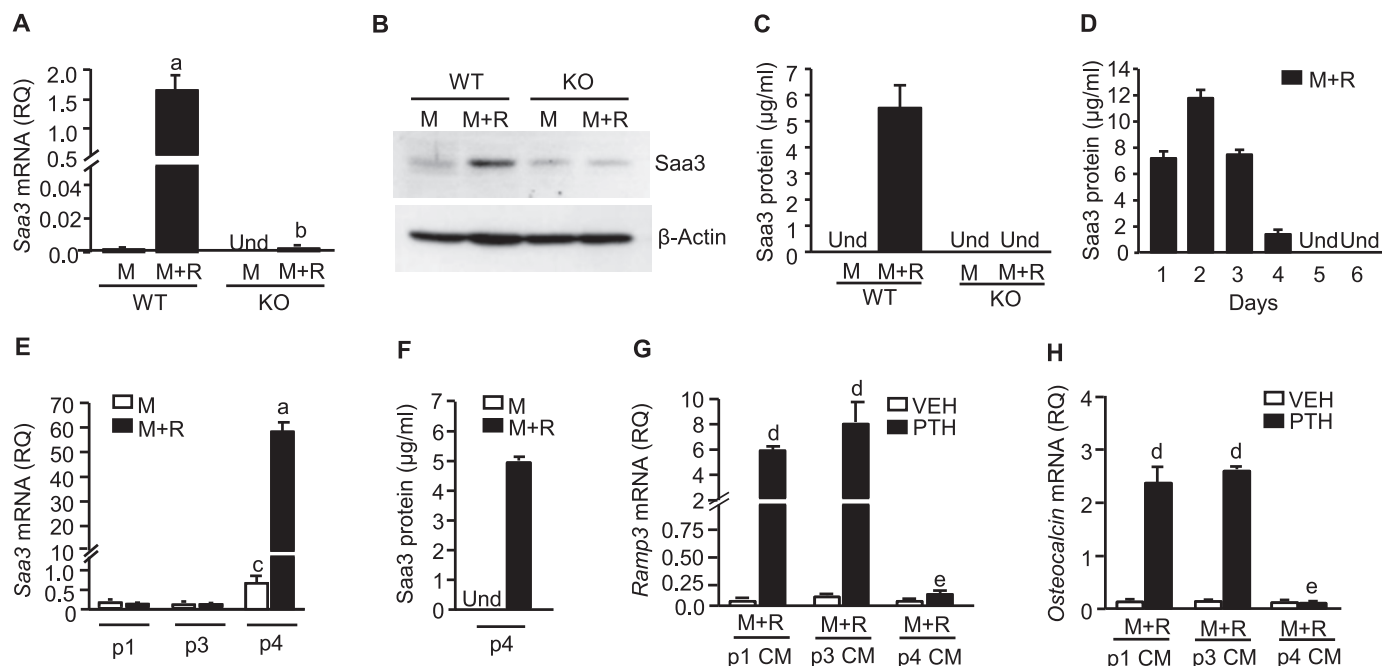


**FIGURE 2. Saa3 was expressed and secreted by RANKL-stimulated preosteoclasts and the CM from RANKL-treated preosteoclasts inhibited PTH-stimulated *Ramp3* expression and osteoblast differentiation.** WT and *Cox2* KO BMMs were treated with M-CSF (M, 30 ng/ml) or M-CSF and RANKL (M+R, each 30 ng/ml) for 1 day before analyzing *Saa3* mRNA by qPCR (A), *Saa3* protein by Western analysis (B), and *Saa3* secreted into the CM by ELISA (C). D, time course study for medium *Saa3* accumulation by ELISA in WT BMMs cultured with M+R. Medium was changed on day 3. E–H, whole marrow from WT mice was sorted for fractions B220<sup>+</sup> CD3<sup>+</sup> (p1) and B220<sup>+</sup> CD3<sup>+</sup> CD11b<sup>low</sup> (p2). Fraction p2 was further sorted for CD115<sup>+</sup> (p3) and CD115<sup>+</sup> (p4). Populations p1, p3, and p4 were plated with M (30 ng/ml) or M+R (30 ng/ml each) and cultured for 3 days to collect RNA and CM. E, *Saa3* mRNA expression by qPCR and F, *Saa3* protein in medium by ELISA. No *Saa3* was detectable in the CM of populations p1 and p3 stimulated with M or M+R. G, *Ramp3* mRNA expression in POBs cultured for 5 days and then given OPG and CM from M+R-treated p1, p3, and p4 populations 1.5 h prior to addition of vehicle or PTH (10 nM) for 3 h. H, *Osteocalcin* mRNA expression in POBs treated with vehicle or PTH in the presence of OPG and CM from M+R-treated p1, p3, and p4 populations for 14 days. Bars are mean  $\pm$  S.E. for  $n = 3$  independent samples, each with 2 technical replicates. Experiments in A and C were performed twice. a, significant effect of RANKL,  $p < 0.01$ . b, significant effect of genotype,  $p < 0.01$ . c, significantly different from M-CSF-stimulated p1 and p3 populations,  $p < 0.01$ . d, significant effect of PTH,  $p < 0.01$ . e, significantly different from CM of other populations,  $p < 0.01$ . RQ, relative quantification values. Und, undetectable.

day 1 of culture was up-regulated only in WT BMMs treated with M-CSF and RANKL (Fig. 2B), and *Saa3* protein was detectable only in the CM from the M-CSF and RANKL-stimulated WT BMMs (Fig. 2C).

The serum amyloid A family in mice consists of three acute phase proteins (*Saa1*, *Saa2*, and *Saa3*) and one constitutively expressed protein (*Saa4*) (25, 26). To determine whether gene expression of the other isoforms was being regulated by RANKL, we measured mRNA expression in BMMs treated with M-CSF alone or M-CSF and RANKL. *Saa3* was the only isoform detectable and induced by RANKL (Table 3). Thus, it is likely that *Saa3* is the predominant *Saa* isoform induced by RANKL.

RANKL drives the commitment of BMMs to the osteoclast lineage and their differentiation into osteoclasts (27). A time course study comparing RANKL-stimulated formation of osteoclast-like cells, defined as TRAP<sup>+</sup> MNCs, and *Saa3* secretion was conducted in WT BMMs. No TRAP<sup>+</sup> MNCs were seen with M-CSF alone, and no *Saa3* was detectable in CM from BMMs treated with M-CSF alone at any time point (data not shown). With RANKL treatment, TRAP<sup>+</sup> MNCs were first observed on day 4 and numbers descended after that (data not shown). *Saa3* protein in the CM was measurable after 12 h of RANKL (data not shown), peaked on day 2, and was undetectable by day 5 (Fig. 2D). Thus, RANKL-stimulated *Saa3* secretion largely occurred before TRAP<sup>+</sup> MNCs were observed, suggesting that the cells secreting *Saa3* could be preosteoclasts.

**TABLE 3**

**mRNA expression (relative quantification values) of the murine *Saa* isoforms measured by qPCR in WT BMMs stimulated with M-CSF (30 ng/ml) or M-CSF + RANKL (30 ng/ml) for 1 day**

Values are mean  $\pm$  S.E. for  $n = 3$  independent samples, each with 2 technical replicates.

Treatments	<i>Saa1</i>	<i>Saa2</i>	<i>Saa3</i>	<i>Saa4</i>
M-CSF	Und <sup>a</sup>	Und	0.94 $\pm$ 0.03	Und
M-CSF + RANKL	Und	Und	46.3 $\pm$ 3.3	Und

<sup>a</sup> Und, undetectable ( $C_t > 33$ ).

**Myeloid Progenitors Committed to the Osteoclast Lineage Secrete *Saa3***—Myeloid progenitors commit to become osteoclasts in response to signals mediated by the receptor for M-CSF, *c-fms*/CD115, and the receptor for RANKL, RANK (28). The marrow fraction designated by CD3<sup>+</sup> B220<sup>+</sup> CD11b<sup>low</sup> CD115<sup>+</sup> contains the population of myeloid cells that commit to become osteoclasts upon RANKL treatment (29, 30). The whole marrow BMM population used in our experiments contains multiple hematopoietic cell types. To confirm the identity of the hematopoietic cell fraction making *Saa3*, whole marrow from WT mice was flow sorted as described under "Experimental Procedures." Population p2 was further sorted into p3 and p4. Populations p1 (B220<sup>+</sup> CD3<sup>+</sup>), p3 (B220<sup>+</sup> CD3<sup>+</sup> CD11b<sup>low</sup> CD115<sup>+</sup>), and p4 (B220<sup>+</sup> CD3<sup>+</sup> CD11b<sup>low</sup> CD115<sup>+</sup>) were collected and grown in the presence of M-CSF or M-CSF and RANKL. On day 4, cells were stained for TRAP. TRAP<sup>+</sup> MNCs were observed only in the p4 population and only with RANKL

treatment (data not shown). On day 3, *Saa3* gene expression was barely detectable in populations p1, p3, and p4 stimulated with M-CSF alone. RANKL induced *Saa3* expression only in population p4 (Fig. 2E). *Saa3* protein secretion in CM was undetectable in populations p1 and p3 stimulated with M-CSF alone or M-CSF plus RANKL (data not shown). *Saa3* protein secretion was also undetectable in the M-CSF alone stimulated population p4. RANKL induced *Saa3* protein secretion only in population p4 (Fig. 2F). CM collected on day 3 from all populations was evaluated for the ability to inhibit PTH-stimulated responses in POBs. Only CM from the RANKL-stimulated p4 population inhibited PTH-stimulated *Ramp3* expression (Fig. 2G) and *Osteocalcin* expression (Fig. 2H) in POBs.

The p4 population is highly enriched in a common monocyte progenitor for bone marrow osteoclasts, macrophages, and dendritic cells (30). Macrophages are not known to be regulated by RANKL, but dendritic cell precursors express RANK and can be regulated by RANKL (31). However, given the correlation of *Saa3* expression with the development of osteoclast-like cells and the lack of media supplements, such as GM-CSF, used to expand dendritic cells in our cultures, it is likely that the cells responsible for the production of *Saa3* in response to RANKL are osteoclast precursors.

**WT BMMs with shRNA Knockdown of *Saa3* Did Not Inhibit PTH-stimulated Responses in POBs**—To determine whether *Saa3* was the inhibitory factor in CM, WT BMMs were transduced with four lentiviral *Saa3* shRNA knockdown vectors and a scrambled lentiviral vector. After 72 h, microscopic evaluation of GFP expression showed BMMs were successfully transduced with all constructs showing grossly similar levels of expression in all the wells (data not shown). RNA, proteins, and CM were collected at 72 h to evaluate the *Saa3* knockdown (Fig. 3, A–C). *Saa3* mRNA expression was decreased 99% in BMMs transduced with two of the shRNA constructs (1 and 2) compared with BMMs transduced with a scrambled control or to a BMM control with no viral transduction (Fig. 3A). On Western blot analysis, *Saa3* protein was not detectable in BMMs transduced with shRNA 1 and 2, whereas no knockdown was observed in BMMs transduced with the scrambled control compared with non-transduced controls (Fig. 3B). Similarly, by ELISA, *Saa3* was secreted into the CM from BMMs with the scrambled control and by non-transduced BMMs but not by BMMs transduced with shRNA 1 or 2 (Fig. 3C).

To examine the effects of *Saa3* knockdown on osteoclastogenesis, BMMs transduced with the scrambled control or with shRNA construct 2 were cultured with RANKL for 6 days (Fig. 3D). Silencing of *Saa3* had no effect on the number or pattern of osteoclastogenesis.

CM collected from BMMs transduced with the shRNA 1 and 2 constructs was added to *Cox2* KO POBs to examine effects on PTH-stimulated cAMP production at 20 min of treatment. As expected, in the absence of any CM, PTH markedly stimulated cAMP production in POBs (Fig. 3, E and F). CM from WT BMMs transduced with the scrambled control, which left *Saa3* expression intact, blocked the effects of PTH, whereas CM from WT BMMs transduced with the shRNA 1 and 2 constructs permitted the PTH stimulation of cAMP. *Ramp3* expression was induced by PTH to similar levels in POBs with

no CM added or with CM from BMMs transduced with the shRNA 1 and 2 constructs but was blocked by CM from BMMs transduced with the scrambled control (data not shown).

To assess the effects of silencing *Saa3* in preosteoclasts, defined as BMMs committed to the osteoclast lineage by treatment with M-CSF and RANKL but not yet forming multinucleated osteoclasts, on PTH-stimulated osteoblastic differentiation, we measured *Osteocalcin* mRNA expression after 14 days of co-culture of POBs with CM (Fig. 3, G and H). The CM was collected from BMM cultures treated for 3 days with M-CSF and RANKL before any TRAP<sup>+</sup> MNCs were observed (Fig. 3D). PTH-stimulated *Osteocalcin* mRNA expression was blocked by CM from BMMs transduced with the scrambled control. There was no inhibition of PTH-stimulated *Osteocalcin* mRNA expression by CM from BMMs transduced with either construct 1 or 2 compared with PTH-stimulated *Osteocalcin* expression in the cultures with no CM.

Co-cultures of POBs and BMMs transduced with the shRNA 2 construct were also done to examine the effects of *Saa3* knockdown in BMMs on PTH-stimulated *Osteocalcin* expression. In this system, PTH induces endogenous RANKL in the POBs, which then drives the BMMs to become osteoclast-like cells (12). Without BMMs, PTH stimulated *Runx2* mRNA, an early marker of osteoblast differentiation, on day 7 of culture and *Osteocalcin* mRNA on day 14 (Fig. 3, I and J). In co-cultures of POBs and non-transduced BMMs or BMMs transduced with a scrambled control, PTH-stimulated *Osteocalcin* expression was blocked. In co-cultures of POBs with BMMs transduced with the shRNA 2 construct, PTH stimulated both *Runx2* and *Osteocalcin* expression. Hence, silencing of *Saa3* in BMMs removed the inhibitory effect of BMMs on PTH-stimulated osteoblast differentiation.

**Recombinant SAA Inhibited PTH-mediated Responses in POBs and the Inhibition Was Blocked by PTX and a Specific Antagonist of the Formyl Peptide Receptor 2 (*Fpr2*)**—Recombinant human SAA, added in the same concentration range as *Saa3* in the CM from RANKL-stimulated WT BMMs (1–10  $\mu$ g/ml), inhibited PTH-stimulated *Ramp3* expression in POBs (Fig. 4A), and SAA at 10  $\mu$ g/ml abrogated the ability of PTH to stimulate cAMP production in POBs (Fig. 4B). SAA (10  $\mu$ g/ml) also blocked PTH-stimulated osteoblastic differentiation as measured by *Osteocalcin* expression, and this inhibition was prevented by PTX (Fig. 4C). Similar to the inhibitory CM, SAA had no effect in the absence of PTH in these experiments.

SAA can act via a number of receptors (32). We examined the possibility that the *Fpr2* receptor mediated the inhibition of PTH-stimulated cAMP signaling by *Saa3*. Murine *Fpr2*, the ortholog of human *FPR2* (formerly called *FPRL1*), is a GPCR that can signal via PTX-sensitive  $G\alpha_{i/o}$  (33, 34). Gene expression of *Fpr2* in POBs grown for 5 days and treated with vehicle, PTH, SAA (10  $\mu$ g/ml), and SAA plus PTH for 3 h did not differ among groups (data not shown). Treatment with a selective agonist for *Fpr2*, WKYMVm, inhibited the stimulatory effect of PTH on *Ramp3* expression in a dose-dependent manner (Fig. 4D). Treatment with a selective antagonist of *Fpr2*, WRW4 (35), reversed the inhibitory effect of exogenous SAA on PTH-stimulated *Ramp3* expression (Fig. 4E). These data suggest

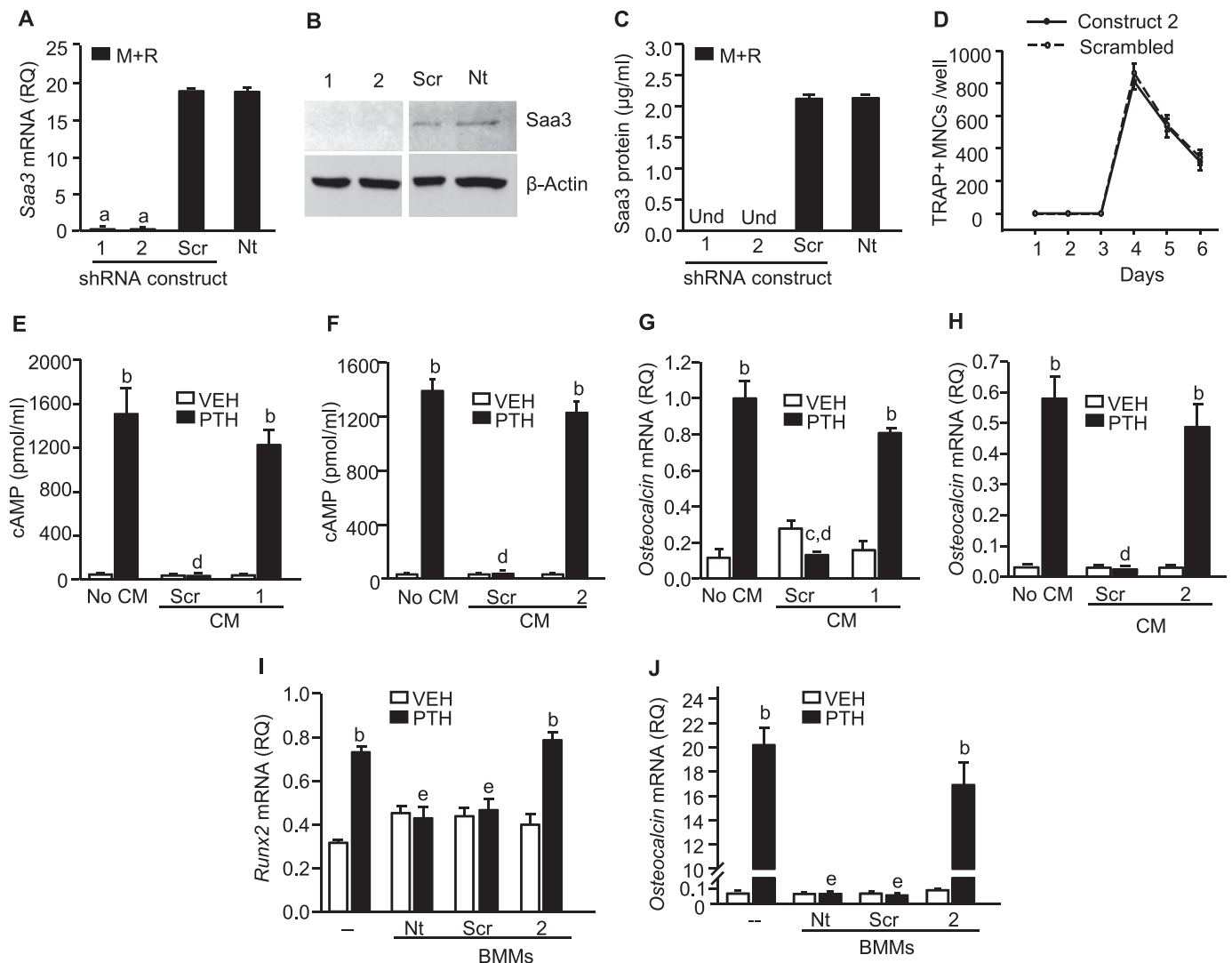


**FIGURE 3. Co-culture of POBs with CM from BMMs with Saa3 silenced or with BMMs themselves did not inhibit PTH-stimulated cAMP production or osteoblast differentiation.** WT BMMs, which were transduced with a scrambled (Scr) control or four different shRNA (1–4) constructs for Saa3 or not transduced at all (Nt), were stimulated with M-CSF (M, 30 ng/ml) or M-CSF plus RANKL (M+R, 30 ng/ml each) for 3 days. M+R-treated BMMs were examined for the knockdown of Saa3, and CM from the Saa3 knockdown was used to treat the POBs. M-treated BMMs were co-cultured with POBs. *A*, Saa3 mRNA expression measured by qPCR in M+R-treated BMMs carrying shRNA 1 or 2 or Scr constructs compared with Nt. *B*, Saa3 protein measured by Western analysis in M+R-treated BMMs carrying shRNA 1 or 2 or Scr constructs compared with Nt. All lanes are a part of one gel. The gel picture was cut to remove constructs that did not knockdown Saa3. There was a gradation in the background density of original gel picture for Saa3 bands; the contrast has not been differentially manipulated. *C*, Saa3 protein concentration in the medium of M+R-treated BMMs measured by ELISA. *D*, time course for TRAP positive (+) MNCs in M+R-treated BMMs carrying Scr or shRNA 2 constructs. CM was collected on day 3 of culture. *E* and *F*, PTH-stimulated cAMP production in POBs grown for 5 days and given no CM or CM from M+R-treated BMMs carrying Scr or shRNA 1 or 2 constructs. CM, OPG, and IBMX (0.5 mM) were added 1.5 h prior to addition of vehicle (VEH) or PTH for 20 min. *G* and *H*, Osteocalcin mRNA in POBs grown for 14 days with OPG, CM, or no CM, VEH, or PTH. *I*, Runx2 mRNA, and *J*, Osteocalcin mRNA in co-cultures of POBs and BMMs at days 7 and 14, respectively. POBs were cultured without BMMs, with un-transduced BMMs, or with BMMs transduced with Scr or shRNA 2 constructs. Bars or symbols are mean  $\pm$  S.E. for  $n = 3$  independent samples, each with 2 technical replicates. Experiments in *A* and *C* were performed twice. *a*, significantly different from Scr or Nt controls,  $p < 0.01$ . *b*, significant effect of PTH,  $p < 0.01$ . *c*,  $p < 0.05$ . *d*, significantly different from no CM or from CM from BMMs with shRNA 1 and 2,  $p < 0.01$ . *e*, significantly different from POBs with no BMMs or POBs with BMMs carrying shRNA 2 construct,  $p < 0.01$ . RQ, relative quantification values. Und, undetectable.

that the inhibitory effect of Saa3 on PTH-stimulated cAMP responses in POBs occurs via Fpr2- $G\alpha_{i/o}$  signaling.

**Continuous PTH *in Vivo* Induced Saa3 Expression**—We previously found that PTH infusion *in vivo* (40  $\mu$ g/kg/days for 12 days) increased trabecular bone mass only in *Cox2* KO mice, not in WT mice, whereas increasing bone resorption equally in WT and KO mice (11). To examine the expression of Saa3 in response to PTH infusion, we measured Saa3 expression in tibial bone, with unflushed marrow, and Saa3 protein in serum at the end of the PTH infusion. Saa3 mRNA expression was

detectable in bone samples but was regulated by PTH only in WT mice where it was induced more than 40-fold (Table 4). Saa3 protein was generally undetectable in serum from *Cox2* KO mice and from vehicle-treated WT mice but was detectable in all serum samples from the PTH-treated WT group. Thus, PTH induced Saa3 expression *in vivo* as well as *in vitro* in a *Cox2*-dependent manner.

The Saa3 induction in tibiae in response to PTH might have reflected expression in osteoblastic or osteoclastic lineage cells. We examined POB cultures differentiated over 3 weeks for reg-

## Saa3 Inhibits PTH Signaling in Osteoblasts

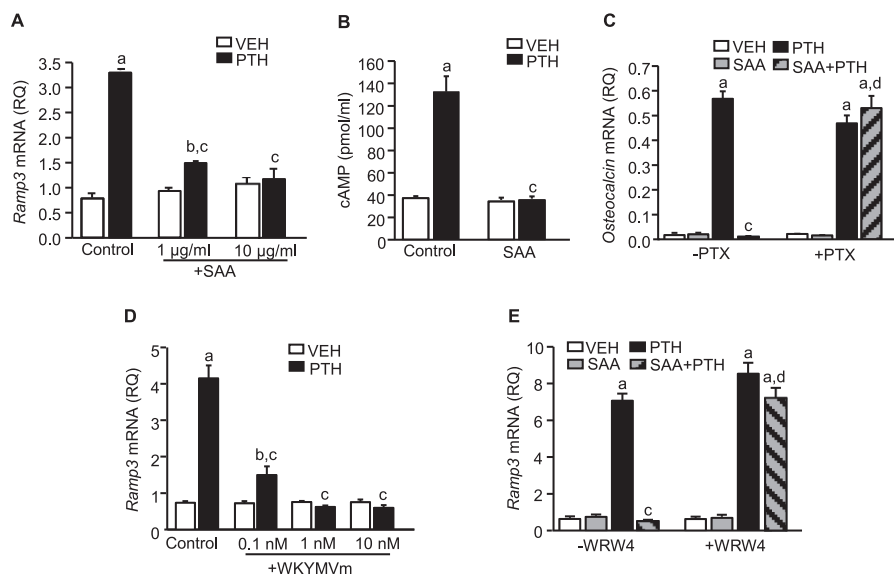


**FIGURE 4. Recombinant SAA inhibited PTH induced cAMP-mediated responses in POBs in a PTX-sensitive manner and the inhibition was blocked by Fpr2 antagonist.** All experiments used *Cox2* KO POBs. For cAMP and *Ramp3* gene expression studies, POBs were cultured for 5 days and then given OPG (50 ng/ml) 1.5 h prior to treatment with PTH ± SAA or PTH ± WKYMVm. **A**, dose-response for the effect of SAA on PTH-stimulated *Ramp3* expression. SAA, 10 µg/ml, was used in future experiments. **B**, effect of SAA on PTH-stimulated cAMP production. IBMX (0.5 mM) was added 1.5 h prior to treatment with vehicle (VEH) or PTH ± SAA for 20 min. **C**, *Osteocalcin* mRNA expression in POBs treated with VEH or PTH ± SAA ± PTX (50 ng/ml) for 14 days. **D**, dose-response for the effect of a selective Fpr2 agonist, WKYMVm, on PTH-stimulated *Ramp3* expression in POBs. WRW4 was added 1.5 h prior to addition of VEH or PTH ± SAA for 3 h. **E**, effect of a selective Fpr2 antagonist, WRW4 (2 µM), on the SAA inhibition of PTH-stimulated *Ramp3* expression in POBs. Bars are mean ± S.E. for *n* = 3 independent samples, each with 2 technical replicates. Experiments in **A** and **C** were performed twice. *a*, significant effect of PTH, *p* < 0.01; *b*, *p* < 0.05. *c*, significant effect of SAA or WKYMVm, *p* < 0.01. *d*, significant effect of PTX or WRW4, *p* < 0.01. RQ, relative quantification values.

**TABLE 4**

**Saa3 gene expression measured by qPCR in unflushed tibia and Saa3 protein expression in serum**

WT and *Cox2* KO mice (3-month-old males) were infused with vehicle or PTH (40 µg/kg/days) for 12 days prior to obtaining serum and dissecting out tibiae. Values are mean ± S.E. from *n* mice.

Tissue	WT mice		<i>Cox2</i> KO mice	
	Vehicle	PTH	Vehicle	PTH
Tibia, mRNA (RQ) <sup>a</sup>	0.086 ± 0.01 <i>n</i> = 7	4.11 ± 0.96 <sup>b</sup> <i>n</i> = 7	0.07 ± 0.01 <i>n</i> = 7	0.19 ± 0.08 <sup>c</sup> <i>n</i> = 7
Serum (µg/ml)	1/5 Detectable	5/5 Detectable	2/5 Detectable	1/4 Detectable
	0.13 <i>n</i> = 5	1.28 ± 0.11 <i>n</i> = 5	0.09, 0.10 <i>n</i> = 5	0.15 <i>n</i> = 4

<sup>a</sup> RQ, relative quantification values.

<sup>b</sup> Significant effect of PTH, *p* ≤ 0.01.

<sup>c</sup> Significant effect of genotype, *p* ≤ 0.01.

ulation of *Saa* isoforms by PTH at days 7, 14, and 21 of culture. *Saa3* was the only isoform detectable, and it was not regulated by PTH (Table 5). These data suggest that PTH induces *Saa3* *in vivo* indirectly via the PTH induction of RANKL in osteoblasts and the subsequent action of RANKL on osteoclast progenitors.

## Discussion

We previously reported that continuous treatment with PTH was unable to stimulate osteoblast differentiation in BMSCs cultured from WT mice but markedly stimulated osteoblast differentiation in *Cox2* KO BMSCs (12, 36). BMSCs contain mesenchymal and hematopoietic precursors that can differentiate into osteoblasts and osteoclasts, respectively. Initially, we also observed the inhibitory effect of *Cox2* expression on PTH-stimulated differentiation in POBs (36) but discovered subsequently that the inhibition was due to hematopoietic cells remaining in the POB cultures. Eventually, we found that CM from WT but not *Cox2* KO BMMs carried an inhibitory factor that blocked PTH-stimulated osteoblast differentiation but had no effect on basal osteoblastic differentiation. The production

of this factor depended on the presence of *Cox2*-produced PGE<sub>2</sub> and on RANKL (12). In the present study, we used CM from RANKL-treated WT and *Cox2* KO BMMs to demonstrate that the inhibitory CM abrogated PTH-stimulated cAMP production and cAMP-mediated gene responses in POBs in a PTX-sensitive manner. We showed that silencing of *Saa3* in BMMs, committed to the osteoclast lineage by RANKL but not yet fused into multinucleated osteoclasts, removed the inhibitory factor from CM. We also showed that BMMs in which *Saa3* was silenced could no longer inhibit PTH-stimulated osteoblast differentiation as measured by *Osteocalcin* mRNA expression. Fig. 5 is a graphic depiction summarizing how we propose that PTH stimulates the production of *Saa3* by preosteoclasts and how *Saa3* can, in turn, inhibit the PTH-cAMP signaling axis, based on our experimental findings.

*Saa3* belongs to a family of highly conserved, acute phase apolipoproteins in vertebrates, whose levels can rise 1000-fold in the circulation during episodes of inflammation, injury, or infection (25, 32, 37). Four genes, *Saa1–4*, exist in mice and four, *SAA1–4*, in humans (25, 38, 39). In the acute phase in

**TABLE 5**

mRNA expression (relative quantification values) of the *Saa* isoforms measured by qPCR in WT POBs stimulated with vehicle or PTH for 7, 14, and 21 days

Values are mean  $\pm$  S.E. for  $n = 3$  independent samples, each with 2 technical replicates.

Day	<i>Saa1</i>		<i>Saa2</i>		<i>Saa3</i>		<i>Saa4</i>	
	Vehicle	PTH	Vehicle	PTH	Vehicle	PTH	Vehicle	PTH
7	Und <sup>a</sup>	Und	Und	Und	0.12 $\pm$ 0.01	0.12 $\pm$ 0.01	Und	Und
14	Und	Und	Und	Und	0.13 $\pm$ 0.00	0.12 $\pm$ 0.02	Und	Und
21	Und	Und	Und	Und	0.13 $\pm$ 0.02	0.13 $\pm$ 0.00	Und	Und

<sup>a</sup> Und, undetectable ( $C_t > 33$ ).

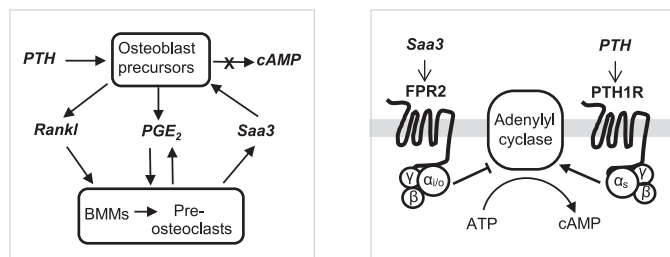


**FIGURE 5. Proposed induction and actions of Saa3.** Left panel, PTH acts on osteoblast precursors to activate cAMP signaling, which ultimately results in osteoblastic differentiation. PTH also induces Rankl and Cox2 expression in osteoblast precursors, and Cox2 then produces PGE<sub>2</sub>. Rankl acts on osteoclast lineage cells (BMMs), committing them to become preosteoclasts and inducing more Cox2/PGE<sub>2</sub>. The combination of RANKL + PGE<sub>2</sub> induces Saa3 in the BMMs/preosteoclasts. Saa3, in turn, is secreted and acts on osteoblast precursors to block PTH-stimulated cAMP production and osteoblastic differentiation. Right panel, PTH and Saa3 act via the GPCRs, PTH1R, and FPR2, respectively. Saa3 activates G $\alpha_{i/o}$  signaling, which blocks the AC conversion of ATP to cAMP that would otherwise be stimulated by PTH-activated G $\alpha_s$  signaling.

mice, *Saa1* and *Saa2* are up-regulated mainly in the liver, whereas *Saa3* is induced in a variety of extra-hepatic tissues, including macrophages and adipocytes (37, 40–42). The individual orthologs can vary greatly in their expression in different species (43). For example, in mice *Saa1*, *Saa2*, and *Saa3* are acute phase inducible genes, whereas *Saa4* is constitutively expressed. In humans, *SAA1* and *SAA2* are inducible, *SAA4* is constitutive, but *SAA3* is a pseudogene. In pigs, *Saa1* is a pseudogene, whereas *Saa3* is highly expressed and inducible (44). SAA is generally considered to be associated with acute and chronic inflammation and was recently reported to activate inflammasomes promoting the production of IL-1 $\beta$  (45, 46). SAA proteins have been implicated in amyloidosis, obesity, rheumatoid arthritis, atherosclerosis, and cancer metastasis (42, 47, 48), suggesting that they might be the connection between chronic inflammation and multiple diseases, but their function is still being debated (44, 49). Although many cytokines have been shown to induce SAA, we believe this is the first report of RANKL induction of Saa3 in preosteoclasts. Bone-resorbing agonists, including PTH, stimulate resorption by inducing RANKL in osteoblast lineage cells; RANKL then binds to RANK on myeloid/monocyte osteoclast progenitors to drive osteoclast formation, differentiation, and activity. Thus, our results suggest a possible means by which bone resorption agonists could contribute to inflammation by inducing Saa3 in preosteoclasts.

PTH is a potent inducer of Cox2, as well as RANKL, in osteoblasts (9). We originally hypothesized that Cox2-produced PGE<sub>2</sub>, which acts via cAMP-mediated signaling similar to PTH and is known to be able to stimulate bone formation (10), might mediate some of the anabolic effects of PTH. Instead, we found,

both *in vitro* (12) and *in vivo* (11, 14), that the osteogenic/anabolic effects of PTH were inhibited in the presence of Cox2 expression. These previous studies indicated that Cox2/PGE<sub>2</sub> was required for the production of the inhibitory factor, and the current study corroborates this requirement for the RANKL production of Saa3 in preosteoclasts. The PGE<sub>2</sub> required for production of Saa3 can be produced by induction of Cox2 in osteoblasts or by the RANKL induction of Cox2 in preosteoclasts (12, 50). Many pro-inflammatory agents and cytokines can induce both Cox2 and RANKL; the subsequent induction of Saa3 could then inhibit cAMP signaling by endogenous PTH and be one means by which inflammation leads to bone loss.

The inhibitory effect of Saa3 on PTH-stimulated cAMP signaling occurred via PTX-sensitive G $\alpha_{i/o}$  signaling, likely mediated by Fpr2. Fpr2 has been discussed as an attractive therapeutic target but it has multiple ligands, stimulates multiple signal transduction pathways, depending on the ligand and the cell type involved, and mediates both pro- and anti-inflammatory responses (51). Several studies in *Fpr2*-deficient mice suggest that *Fpr2* deficiency can worsen inflammation and tumorigenesis (52–54). Hence, it might be best to target the ligand rather than receptor.

Other studies have shown that activation of G $\alpha_i$ -coupled signaling can lead to bone loss. Transgenic expression of a constitutively active G $\alpha_i$ -coupled GPCR in osteoblasts led to marked trabecular osteopenia (55). Osteoblast-specific expression of the catalytic subunit of PTX *in vivo* resulted in site-specific increases in cortical and trabecular bone, but the phenotype was complex (56). These two studies did not find any effect of activation of G $\alpha_i$ -coupled signaling in osteoblasts *in vitro* despite significant *in vivo* phenotypes. The authors suggested that some component of the bone microenvironment that was necessary for manifestation of the phenotypes *in vivo* was missing from the *in vitro* culture systems. Perhaps the missing component *in vitro* was PTH and the bone loss *in vivo* was due to the inhibition of endogenous PTH-driven bone responses by activated G $\alpha_{i/o}$  signaling.

Our previous study showed that the inhibition of PTH-stimulated osteoblastic differentiation required the presence of hematopoietic lineage cells or CM from RANKL-treated BMMs and could be blocked by OPG (12). In the current study, we show that Saa3 is the inhibitory factor secreted in response to RANKL acting on BMMs or preosteoclasts. This has led us to propose that PTH induces Saa3 production indirectly by stimulating RANKL expression in osteoblast lineage cells that then acts on preosteoclasts to stimulate Saa3 secretion. It is unclear if Saa produced by osteoblast lineage cells also has a role in regulating osteoblastic function. *SAA1/2* transcripts have been

found in human bone and osteosarcoma cell lines (57). A recent study reported that *Saa3* was expressed in osteoblastic lineage cells, particularly as they terminally differentiated into the osteocyte phenotype, and that recombinant Saa3 inhibited osteoblastic differentiation and stimulated osteoclastic differentiation (58). In our study, *Saa1/2* transcripts in POBs differentiated for 1–3 weeks were not detectable; *Saa3* mRNA expression in POBs was unchanged with differentiation and not regulated by PTH; and neither CM containing Saa3 nor recombinant SAA had any effect on cAMP responses or differentiation in vehicle-treated POBs. In addition, osteoclast formation in BMMs was not affected by silencing of Saa3. The differences between our studies might be due to the use of different cell models.

In summary, Saa3 is a novel means by which preosteoclasts can inhibit PTH-stimulated cAMP-mediated responses. There are a number of studies showing soluble factors produced by non-resorbing osteoclasts that can stimulate osteoblast differentiation (59–62) or inhibit differentiation (60, 63, 64), but we believe this is the first factor shown to have an inhibitory effect on PTH-stimulated osteoblast differentiation but not on vehicle-treated osteoblasts. Because PTH is a critical regulator of bone turnover as well as an important anabolic drug for treating osteoporosis and because aging is characterized by chronic inflammation and bone loss, inhibition of Saa3 may become a new target for treating osteoporosis. There are multiple potential ways to inhibit Saa3 production by preosteoclasts, including inhibitors of osteoclast formation, such as anti-RANKL and OPG, and inhibitors of Cox2 activity or PGE<sub>2</sub> receptors. The dependence of Saa3 production on Cox2/PGE<sub>2</sub> fits well with the status of PGE<sub>2</sub> as an inflammatory mediator that promotes tumorigenesis (65), and direct inhibition of SAA might be a way to limit the inflammatory effects of PGE<sub>2</sub> without the added complications of inhibiting all PGE<sub>2</sub> activity.

**Author Contributions**—S. C. and C. P. conceived the study, designed the experiments, and wrote the paper. Experiments were performed by S. C., A. G., C. J., and T. E. S. C., C. P., T. E., A. G., and C. J. analyzed the data. H. A., J. L., and A. G. critically reviewed the data and contributed important intellectual content. All authors reviewed the paper and approved the final version of the paper.

**Acknowledgments**—We thank Dr. Evan Jellison from the flow cytometry facility and Anupinder Kaur from the microarray facility at the University of Connecticut Health for their expert technical support.

## References

- Silva, B. C., and Bilezikian, J. P. (2015) Parathyroid hormone: anabolic and catabolic actions on the skeleton. *Curr. Opin. Pharmacol.* **22**, 41–50
- Yang, D., Singh, R., Divieti, P., Guo, J., Bouxsein, M. L., and Bringham, F. R. (2007) Contributions of parathyroid hormone (PTH)/PTH-related peptide receptor signaling pathways to the anabolic effect of PTH on bone. *Bone* **40**, 1453–1461
- Takahashi, N., Maeda, K., Ishihara, A., Uehara, S., and Kobayashi, Y. (2011) Regulatory mechanism of osteoclastogenesis by RANKL and Wnt signals. *Front. Biosci. (Landmark Ed)* **16**, 21–30
- Baron, R., and Hesse, E. (2012) Update on bone anabolics in osteoporosis treatment: rationale, current status, and perspectives. *J. Clin. Endocrinol. Metab.* **97**, 311–325
- Augustine, M., and Horwitz, M. J. (2013) Parathyroid hormone and para-

- thyroid hormone-related protein analogs as therapies for osteoporosis. *Curr. Osteoporos. Rep.* **11**, 400–406
- Iida-Klein, A., Lu, S. S., Kapadia, R., Burkhart, M., Moreno, A., Dempster, D. W., and Lindsay, R. (2005) Short-term continuous infusion of human parathyroid hormone 1–34 fragment is catabolic with decreased trabecular connectivity density accompanied by hypercalcemia in C57BL/6 mice. *J. Endocrinol.* **186**, 549–557
- Horwitz, M. J., Tedesco, M. B., Sereika, S. M., Prebehala, L., Gundberg, C. M., Hollis, B. W., Bisello, A., Garcia-Ocana, A., Carneiro, R. M., and Stewart, A. F. (2011) A 7-day continuous infusion of PTH or PTHrP suppresses bone formation and uncouples bone turnover. *J. Bone Miner. Res.* **26**, 2287–2297
- Robling, A. G., Kedlaya, R., Ellis, S. N., Childress, P. J., Bidwell, J. P., Bellido, T., and Turner, C. H. (2011) Anabolic and catabolic regimens of human parathyroid hormone 1–34 elicit bone- and envelope-specific attenuation of skeletal effects in Sost-deficient mice. *Endocrinology* **152**, 2963–2975
- Pilbeam, C. C., Choudhary, S., Blackwell, K. A., and Raisz, L. G. (2008) Prostaglandins and Bone Metabolism. In Bilezikian, J. P., Raisz, L. G., and Martin, T. J. (eds) *Principles of Bone Biology*, pp. 1235–1271, Elsevier/Academic Press, San Diego
- Blackwell, K. A., Raisz, L. G., and Pilbeam, C. C. (2010) Prostaglandins in bone: bad cop, good cop? *Trends Endocrinol. Metab.* **21**, 294–301
- Choudhary, S., Canalis, E., Estus, T., Adams, D., and Pilbeam, C. (2015) Cyclooxygenase-2 suppresses the anabolic response to PTH infusion in mice. *PLoS ONE* **10**, e0120164
- Choudhary, S., Blackwell, K., Voznesensky, O., Deb Roy, A., and Pilbeam, C. (2013) Prostaglandin E<sub>2</sub> acts via bone marrow macrophages to block PTH-stimulated osteoblast differentiation *in vitro*. *Bone* **56**, 31–41
- Morham, S. G., Langenbach, R., Loftin, C. D., Tian, H. F., Vouloumanos, N., Jennette, J. C., Mahler, J. F., Kluckman, K. D., Ledford, A., Lee, C. A., and Smithies, O. (1995) Prostaglandin synthase 2 gene disruption causes severe renal pathology in the mouse. *Cell* **83**, 473–482
- Xu, M., Choudhary, S., Voznesensky, O., Gao, Q., Adams, D., Diaz-Doran, V., Wu, Q., Goltzman, D., Raisz, L. G., and Pilbeam, C. C. (2010) Basal bone phenotype and increased anabolic responses to intermittent parathyroid hormone in healthy male COX-2 knockout mice. *Bone* **47**, 341–352
- Jacome-Galarza, C. E., Lee, S. K., Lorenzo, J. A., and Aguila, H. L. (2011) Parathyroid hormone regulates the distribution and osteoclastogenic potential of hematopoietic progenitors in the bone marrow. *J. Bone Miner. Res.* **26**, 1207–1216
- Lee, S. K., and Lorenzo, J. A. (2002) Regulation of receptor activator of nuclear factor- $\kappa$ B ligand and osteoprotegerin mRNA expression by parathyroid hormone is predominantly mediated by the protein kinase a pathway in murine bone marrow cultures. *Bone* **31**, 252–259
- Li, X., Liu, H., Qin, L., Tamasi, J., Bergenstock, M., Shapses, S., Feyen, J. H., Notterman, D. A., and Partridge, N. C. (2007) Determination of dual effects of parathyroid hormone on skeletal gene expression *in vivo* by microarray and network analysis. *J. Biol. Chem.* **282**, 33086–33097
- Phelps, E., Bezouglaia, O., Tetradis, S., and Nervina, J. M. (2005) Parathyroid hormone induces receptor activity modifying protein-3 (RAMP3) expression primarily via 3',5'-cyclic adenosine monophosphate signaling in osteoblasts. *Calcif. Tissue Int.* **77**, 96–103
- McCauley, L. K., Koh, A. J., Beecher, C. A., and Rosol, T. J. (1997) Proto-oncogene *c-fos* is transcriptionally regulated by parathyroid hormone (PTH) and PTH-related protein in a cyclic adenosine monophosphate-dependent manner in osteoblastic cells. *Endocrinology* **138**, 5427–5433
- Tetradis, S., Bezouglaia, O., and Tsingotjidou, A. (2001) Parathyroid hormone induces expression of the nuclear orphan receptor Nurr1 in bone cells. *Endocrinology* **142**, 663–670
- Tang, W. J., and Hurley, J. H. (1998) Catalytic mechanism and regulation of mammalian adenylyl cyclases. *Mol. Pharmacol.* **54**, 231–240
- Sadana, R., and Dessauer, C. W. (2009) Physiological roles for G protein-regulated adenylyl cyclase isoforms: insights from knockout and overexpression studies. *Neurosignals* **17**, 5–22
- Fields, T. A., and Casey, P. J. (1997) Signalling functions and biochemical properties of pertussis toxin-resistant G-proteins. *Biochem. J.* **321**, 561–571

24. Taussig, R., Tang, W. J., Hepler, J. R., and Gilman, A. G. (1994) Distinct patterns of bidirectional regulation of mammalian adenylyl cyclases. *J. Biol. Chem.* **269**, 6093–6100
25. Uhlir, C. M., and Whitehead, A. S. (1999) Serum amyloid A, the major vertebrate acute-phase reactant. *Eur. J. Biochem.* **265**, 501–523
26. Thorn, C. F., and Whitehead, A. S. (2002) Differential transcription of the mouse acute phase serum amyloid A genes in response to pro-inflammatory cytokines. *Amyloid* **9**, 229–236
27. Boyce, B. F., and Xing, L. (2008) Functions of RANKL/RANK/OPG in bone modeling and remodeling. *Arch. Biochem. Biophys.* **473**, 139–146
28. Arai, F., Miyamoto, T., Ohneda, O., Inada, T., Sudo, T., Brasel, K., Miyata, T., Anderson, D. M., and Suda, T. (1999) Commitment and differentiation of osteoclast precursor cells by the sequential expression of c-Fms and receptor activator of nuclear factor  $\kappa$ B (RANK) receptors. *J. Exp. Med.* **190**, 1741–1754
29. Jacquin, C., Gran, D. E., Lee, S. K., Lorenzo, J. A., and Aguila, H. L. (2006) Identification of multiple osteoclast precursor populations in murine bone marrow. *J. Bone Miner. Res.* **21**, 67–77
30. Jacome-Galarza, C. E., Lee, S. K., Lorenzo, J. A., and Aguila, H. L. (2013) Identification, characterization, and isolation of a common progenitor for osteoclasts, macrophages, and dendritic cells from murine bone marrow and periphery. *J. Bone Miner. Res.* **28**, 1203–1213
31. Kinugawa, S., Koide, M., Kobayashi, Y., Mizoguchi, T., Ninomiya, T., Muto, A., Kawahara, I., Nakamura, M., Yasuda, H., Takahashi, N., and Udagawa, N. (2012) Tetracyclines convert the osteoclastic-differentiation pathway of progenitor cells to produce dendritic cell-like cells. *J. Immunol.* **188**, 1772–1781
32. Ye, R. D., and Sun, L. (2015) Emerging functions of serum amyloid A in inflammation. *J. Leukoc. Biol.* **98**, 923–929
33. Migeotte, L., Communi, D., and Parmentier, M. (2006) Formyl peptide receptors: a promiscuous subfamily of G protein-coupled receptors controlling immune responses. *Cytokine Growth Factor Rev.* **17**, 501–519
34. Lee, H. Y., Kim, S. D., Shim, J. W., Kim, H. J., Yun, J., Baek, S. H., Kim, K., and Bae, Y. S. (2010) A pertussis toxin sensitive G-protein-independent pathway is involved in serum amyloid A-induced formyl peptide receptor 2-mediated CCL2 production. *Exp. Mol. Med.* **42**, 302–309
35. Bae, Y. S., Lee, H. Y., Jo, E. J., Kim, J. I., Kang, H. K., Ye, R. D., Kwak, J. Y., and Ryu, S. H. (2004) Identification of peptides that antagonize formyl peptide receptor-like 1-mediated signaling. *J. Immunol.* **173**, 607–614
36. Choudhary, S., Huang, H., Raisz, L., and Pilbeam, C. (2008) Anabolic effects of PTH in cyclooxygenase-2 knockout osteoblasts *in vitro*. *Biochem. Biophys. Res. Commun.* **372**, 536–541
37. Meek, R. L., Eriksen, N., and Benditt, E. P. (1992) Murine serum amyloid A3 is a high density apolipoprotein and is secreted by macrophages. *Proc. Natl. Acad. Sci. U.S.A.* **89**, 7949–7952
38. Sellar, G. C., Oghene, K., Boyle, S., Bickmore, W. A., and Whitehead, A. S. (1994) Organization of the region encompassing the human serum amyloid A (SAA) gene family on chromosome 11p15.1. *Genomics* **23**, 492–495
39. Sipe, J. (1999) Revised nomenclature for serum amyloid A (SAA) Nomenclature Committee of the International Society of Amyloidosis: part 2. *Amyloid* **6**, 67–70
40. Reigstad, C. S., Lundén, G. O., Felin, J., and Bäckhed, F. (2009) Regulation of serum amyloid A3 (SAA3) in mouse colonic epithelium and adipose tissue by the intestinal microbiota. *PLoS ONE* **4**, e5842
41. Son, D. S., Terranova, P. F., and Roby, K. F. (2010) Interaction of adenosine 3',5'-cyclic monophosphate and tumor necrosis factor- $\alpha$  on serum amyloid A3 expression in mouse granulosa cells: dependence on CCAAT-enhancing binding protein- $\beta$  isoform. *Endocrinology* **151**, 3407–3419
42. den Hartigh, L. J., Wang, S., Goodspeed, L., Ding, Y., Averill, M., Subramanian, S., Wietecha, T., O'Brien, K. D., and Chait, A. (2014) Deletion of serum amyloid A3 improves high fat high sucrose diet-induced adipose tissue inflammation and hyperlipidemia in female mice. *PLoS ONE* **9**, e108564
43. Uhlir, C. M., Burgess, C. J., Sharp, P. M., and Whitehead, A. S. (1994) Evolution of the serum amyloid A (SAA) protein superfamily. *Genomics* **19**, 228–235
44. Olsen, H. G., Skovgaard, K., Nielsen, O. L., Leifsson, P. S., Jensen, H. E., Iburg, T., and Heegaard, P. M. (2013) Organization and biology of the porcine serum amyloid A (SAA) gene cluster: isoform specific responses to bacterial infection. *PLoS ONE* **8**, e76695
45. Niemi, K., Teirilä, L., Lappalainen, J., Rajamäki, K., Baumann, M. H., Öörni, K., Wolff, H., Kovanen, P. T., Matikainen, S., and Eklund, K. K. (2011) Serum amyloid A activates the NLRP3 inflammasome via P2X7 receptor and a cathepsin B-sensitive pathway. *J. Immunol.* **186**, 6119–6128
46. Migita, K., Izumi, Y., Jiuchi, Y., Kozuru, H., Kawahara, C., Nakamura, M., Nakamura, T., Agematsu, K., Masumoto, J., Yasunami, M., Kawakami, A., and Eguchi, K. (2014) Serum amyloid A induces NLRP-3-mediated IL-1 $\beta$  secretion in neutrophils. *PLoS ONE* **9**, e96703
47. Hiratsuka, S., Watanabe, A., Sakurai, Y., Akashi-Takamura, S., Ishibashi, S., Miyake, K., Shibuya, M., Akira, S., Aburatani, H., and Maru, Y. (2008) The S100A8-serum amyloid A3-TLR4 paracrine cascade establishes a pre-metastatic phase. *Nat. Cell Biol.* **10**, 1349–1355
48. Eklund, K. K., Niemi, K., and Kovanen, P. T. (2012) Immune functions of serum amyloid A. *Crit. Rev. Immunol.* **32**, 335–348
49. Kisilevsky, R., and Manley, P. N. (2012) Acute-phase serum amyloid A: perspectives on its physiological and pathological roles. *Amyloid* **19**, 5–14
50. Han, S. Y., Lee, N. K., Kim, K. H., Jang, I. W., Yim, M., Kim, J. H., Lee, W. J., and Lee, S. Y. (2005) Transcriptional induction of cyclooxygenase-2 in osteoclast precursors is involved in RANKL-induced osteoclastogenesis. *Blood* **106**, 1240–1245
51. Cattaneo, F., Parisi, M., and Ammendola, R. (2013) Distinct signaling cascades elicited by different formyl peptide receptor 2 (FPR2) agonists. *Int. J. Mol. Sci.* **14**, 7193–7230
52. Chen, K., Liu, M., Liu, Y., Yoshimura, T., Shen, W., Le, Y., Durum, S., Gong, W., Wang, C., Gao, J. L., Murphy, P. M., and Wang, J. M. (2013) Formylpeptide receptor-2 contributes to colonic epithelial homeostasis, inflammation, and tumorigenesis. *J. Clin. Invest.* **123**, 1694–1704
53. Giebler, A., Streetz, K. L., Soehnlein, O., Neumann, U., Wang, J. M., and Brandenburg, L. O. (2014) Deficiency of formyl peptide receptor 1 and 2 is associated with increased inflammation and enhanced liver injury after LPS-stimulation. *PLoS ONE* **9**, e100522
54. Oldekamp, S., Pscheidt, S., Kress, E., Soehnlein, O., Jansen, S., Pufe, T., Wang, J. M., Tauber, S. C., and Brandenburg, L. O. (2014) Lack of formyl peptide receptor 1 and 2 leads to more severe inflammation and higher mortality in mice with of pneumococcal meningitis. *Immunology* **143**, 447–461
55. Peng, J., Bencsik, M., Louie, A., Lu, W., Millard, S., Nguyen, P., Burghardt, A., Majumdar, S., Wronski, T. J., Halloran, B., Conklin, B. R., and Nissenson, R. A. (2008) Conditional expression of a G $\gamma$ -coupled receptor in osteoblasts results in trabecular osteopenia. *Endocrinology* **149**, 1329–1337
56. Millard, S. M., Louie, A. M., Wattanachanya, L., Wronski, T. J., Conklin, B. R., and Nissenson, R. A. (2011) Blockade of receptor-activated G $\gamma$  signaling in osteoblasts *in vivo* leads to site-specific increases in cortical and cancellous bone formation. *J. Bone Miner. Res.* **26**, 822–832
57. Kovacevic, A., Hammer, A., Stadelmeier, E., Windischhofer, W., Sundl, M., Ray, A., Schweighofer, N., Friedl, G., Windhager, R., Sattler, W., and Malle, E. (2008) Expression of serum amyloid A transcripts in human bone tissues, differentiated osteoblast-like stem cells and human osteosarcoma cell lines. *J. Cell Biochem.* **103**, 994–1004
58. Thaler, R., Sturmlechner, I., Spitzer, S., Riester, S. M., Rumpler, M., Zwierina, J., Klaushofer, K., van Wijnen, A. J., and Varga, F. (2015) Acute-phase protein serum amyloid A3 is a novel paracrine coupling factor that controls bone homeostasis. *FASEB J.* **29**, 1344–1359
59. Karsdal, M. A., Martin, T. J., Bollerslev, J., Christiansen, C., and Henriksen, K. (2007) Are nonresorbing osteoclasts sources of bone anabolic activity? *J. Bone Miner. Res.* **22**, 487–494
60. Pederson, L., Ruan, M., Westendorf, J. J., Khosla, S., and Oursler, M. J. (2008) Regulation of bone formation by osteoclasts involves Wnt/BMP signaling and the chemokine sphingosine-1-phosphate. *Proc. Natl. Acad. Sci. U.S.A.* **105**, 20764–20769
61. Kreja, L., Brenner, R. E., Tautzenberger, A., Liedert, A., Friemert, B., Ehrnthaller, C., Huber-Lang, M., and Ignatius, A. (2010) Non-resorbing osteoclasts induce migration and osteogenic differentiation of mesenchymal stem cells. *J. Cell Biochem.* **109**, 347–355

## ***Saa3 Inhibits PTH Signaling in Osteoblasts***

62. Henriksen, K., Andreassen, K. V., Thudium, C. S., Gudmann, K. N., Moscatelli, I., Crüger-Hansen, C. E., Schulz, A. S., Dziegiel, M. H., Richter, J., Karsdal, M. A., and Neutzsky-Wulff, A. V. (2012) A specific subtype of osteoclasts secretes factors inducing nodule formation by osteoblasts. *Bone* **51**, 353–361
63. Walker, E. C., McGregor, N. E., Poulton, I. J., Pompolo, S., Allan, E. H., Quinn, J. M., Gillespie, M. T., Martin, T. J., and Sims, N. A. (2008) Car-diotrophin-1 is an osteoclast-derived stimulus of bone formation required for normal bone remodeling. *J. Bone Miner. Res.* **23**, 2025–2032
64. Negishi-Koga, T., Shinohara, M., Komatsu, N., Bito, H., Kodama, T., Friedel, R. H., and Takayanagi, H. (2011) Suppression of bone formation by osteoclastic expression of semaphorin 4D. *Nat. Med.* **17**, 1473–1480
65. Wang, D., and DuBois, R. N. (2013) An inflammatory mediator, prostaglandin E2, in colorectal cancer. *Cancer J.* **19**, 502–510